Int. J. Heat Mass Transfer. Vol. 24, No. 5, pp. 933–944, 1981
Printed in Great Britain

0017–9310/81/050933–12 $02.00/0

FINITE AMPLITUDE CONVECTION IN INCLINED AND VERTICAL SLOTS —A POWER INTEGRAL ANALYSIS

DOUGLAS W. RUTH
Department of Mechanical Engineering, University of Calgary, Calgary, Alberta, Canada

(*Received* 3 *December* 1979 *and in revised form* 20 *November* 1980)

Abstract—A power integral analysis is performed to study the effect of angle and Prandtl number on the heat transfer just after the convective instability in inclined and vertical fluid layers. The form of convection is assumed to be transverse rolls. The energetics of the instability are shown to be in good agreement with those published by Hart. The variation of the energetics with Prandtl number are used to explain the variation of the critical Grashof number with Prandtl number. The heat transfer results are shown to be in good agreement with some of the data of Konicek and with the theoretical work of Gotoh and Ikeda. These results suggest that the vertical temperature gradient observed in vertical fluid layers may not be as important in layers inclined at $\phi \leq 80°$. The effect of the instability on the heat transfer is shown to decrease as $\phi \to 90°$ and $Pr \to 10$.

NOMENCLATURE

A_i,	amplitudes;
c_i,	constants;
E_i,	energetics;
F,	U, W, θ;
f,	u, w, T or P;
Gr,	Grashof number;
I_i,	values of integrals;
P,	pressure;
Pr,	Prandtl number;
x, y, z,	spatial coordinates;
S_i,	constants;
T,	temperature;
t,	time;
U, W,	dependence of u' and w' on z;
u, v, w,	velocities.

Greek symbols

α,	spatial wave number;
ϕ,	angle;
θ,	dependence of T' on z;
η, ξ,	integration limits.

Subscripts

a,	average;
b,	base;
c,	critical.

Superscript

$'$,	fluctuating component.

1. INTRODUCTION

1.1. *The problem*

THIS paper describes results of a study of finite amplitude convection in inclined and vertical, infinitely long slots. The present work is closely related to the author's previous work on the stability of the conduction regime [1, 2]; the reader is referred to this previous work for a detailed description of the problem. The heat transfer in the region just after the transition from the conduction regime to the multicellular convection regime is the subject of the present paper, with exclusive consideration given to transitions resulting in transverse rolls. The method of determining the heat transfer is the well-known power integral technique.

1.2. *The relevant literature*

There has been considerable interest in the heat transfer between parallel plates in inclined and vertical positions; both theoretical and experimental results are available in the literature. However, most of these studies are not relevant to the present work because they consider layers which do not behave as if they are infinite in the lateral plane or they consider flow regimes far from the point of the original instability. It has been determined both experimentally (e.g. Eckert and Carlson [3], Elder [4], Hart [5]) and theoretically (e.g. Gill [6], Raithby, Hollands and Unny [7]) that, in a vertical layer, provided the layer is of finite length, a vertical temperature gradient will always exist in the central region (core) of the layer. This gradient has been taken into account, in many stability studies, by assuming a base solution first proposed by Elder. It is important to keep in mind that, although Elder's base solution accounts for the vertical temperature gradient, it does not satisfy the isothermal boundary conditions. The most recent and comprehensive study utilizing Elder's base solution is due to Bergholz [8]. When the isothermal boundary problem is explicitly considered, it is not clear whether it is more appropriate to ignore the vertical temperature gradient, or to consider a base solution which does not satisfy all the boundary conditions. Undoubtedly neither method will yield consistently correct results. The present work

does not take the vertical gradient into account.

There are only two works which deal with finite amplitude convection near the instability point for transverse rolls in inclined and vertical layers. The first of these is the experimental work of Konicek [9] which gives heat transfer data for air ($Pr = 0.71$) at the angles $\phi = 75°, 80°, 85°$ and $90°$ and for $Ra_c \leq Ra \leq 10^5$. The aspect ratio of these experiments was 48. The second is a theoretical study by Gotoh and Ikeda [10] which gives theoretical predictions of the heat transfer for $\phi = 90°$ and $Pr = 7.5$ (i.e. water). It has been shown (see [2]) that Konicek's transverse roll data [9] agree with the stability criteria predicted from linear stability theory for only the lower angles (i.e. $\phi = 75°$ and $80°$) and not for angles of $85°$ and $90°$. The presumed reason for this is that the vertical temperature gradient, which was not included in the linear stability theory, dominates at higher angles. The work of Gotoh and Ikeda [10], although containing but one result, is closely akin to the present work in that it was done by means of the power integral technique; the major difference between the two studies lies in the method of applying this technique.

The basis of the current work is the combination of the power series stability solutions, as presented in [1], with the power integral technique, to obtain information on the heat transfer in the region just after the onset of multi-cellular convection (the power integral technique as applied in [10] made use of solutions obtained by numerical integration using the Runge–Kutta–Gill method). Since power series are easily manipulated on a computer, the various multiplications and integrations necessary in the power integral technique were efficiently obtained. This allowed a large range of the parameters ϕ and Pr to be considered in the present study.

1.3. *Aims of the present work*

The aims of the work presented in this paper were:

(a) to develop an analytical technique which would be useful for determining the physical importance, in terms of heat transfer, of conduction regime instabilities;

(b) to provide a comprehensive energetics analysis of the transition mechanism, and;

(c) to analyse the effect of ϕ and Pr on the relative importance of the transition to multi-cellular convection in inclined and vertical fluid layers.

2. POWER INTEGRAL TECHNIQUE

The relevant governing equations for convective heating in an inclined or vertical slot admit a base solution, that is, a solution which allows for heating by conduction only. If the transition from this conduction regime to the multi-cellular convection regime results in steady rolls whose axes are in the y(cross-slope) direction, the variables in the governing equation may be expressed as

$$u = u_b + u_a(z) + A_x u'(x, z) \tag{1a}$$

$$v = 0 \tag{1b}$$

$$w = A_z w'(x, z) \tag{1c}$$

$$P = P_b + P_a(z) + A_p P'(x, z) \tag{1d}$$

and

$$T = T_b + T_a(z) + A_T T'(x, z) \tag{1e}$$

where x is the up-slope coordinate and z is the cross-stream coordinate. The subscript b denotes the base solution, the subscript a denotes a spatially averaged quantity (averaged over x), A_x, A_z, A_T and A_P denote amplitudes; and u', w', T' and P' denote functional forms, periodic in x, and as yet unspecified.

The power integral technique now proceeds as follows:

(1) Equations 1 are substituted into the governing equations.

(2) The resultant equations are averaged over x.

(3) These averaged equations are solved to yield

$$T_a = Pr\, A_T A_z \left\{ \int_0^z \langle T'w' \rangle \, dz - z \int_{-1/2}^{1/2} \langle T'w' \rangle \, dz \right\} \tag{2a}$$

and

$$\begin{aligned} v_a = {} & A_x A_z \left\{ \int_0^z \langle u'w' \rangle \, dz - z \int_{-1/2}^{1/2} \langle u'w' \rangle \, dz \right\} \\ & - PrGr \sin\phi \, A_T A_z \left\{ \int_0^z \int_0^\xi \int_0^\eta \langle T'w' \rangle \, d\eta \, d\xi \, dz \right. \\ & - z \int_{-1/2}^{1/2} \int_0^\xi \int_0^\eta \langle T'w' \rangle \, d\eta \, d\xi \, dz \\ & \left. - \left[\frac{z^3}{6} - \frac{z}{24} \right] \int_{-1/2}^{1/2} \langle T'w' \rangle \, dz \right\} \end{aligned} \tag{2b}$$

where $\langle \ \rangle$ denotes an average over x, and ϕ is the angle of the layer measured from the horizontal.

(4) The averaged equations are subtracted from the governing equations to yield the 'fluctuation' equations.

(5) The fluctuation equations are orthogonalized over x and z, the momentum equations with u' and w' and the energy equation with T'. After considerable algebra, which makes use of boundary conditions and the periodicity of u', w' and T', the following equations result

$$A_x \frac{\partial u'}{\partial x} + A_z \frac{\partial w'}{\partial z} = 0 \tag{3a}$$

$$\begin{aligned} \langle\langle & A_z u'w' \frac{d(u_b + u_a)}{dz} + A_x \left\{ \left(\frac{\partial u'}{\partial x} \right)^2 + \left(\frac{\partial u'}{\partial z} \right)^2 \right\} \\ & + A_z \left\{ \left(\frac{\partial w'}{\partial x} \right)^2 + \left(\frac{\partial w'}{\partial z} \right)^2 \right\} + A_p \left(u' \frac{\partial P'}{\partial x} + w' \frac{\partial P'}{\partial z} \right) \\ & - Gr\, A_T (\sin\phi \, u'T' + \cos\phi \, w'T') \rangle\rangle = 0 \end{aligned} \tag{3b}$$

and

$$\langle\langle PrA_z w'T' \frac{d(T_b + T_a)}{dz} + A_T \times \left\{\left(\frac{\partial T'}{\partial x}\right)^2 + \left(\frac{\partial T'}{\partial z}\right)^2\right\}\rangle\rangle = 0 \quad (3c)$$

where $\langle\langle\ \rangle\rangle$ denotes an average over x and z. Equations (3) are algebraic expressions for A_x, A_z and A_T. If the true forms of u', w', T' and P' were known, equations (3) could be solved for the exact values of these amplitudes.

By applying Stuart's [11] shape assumption, the primed quantities are now identified with the solutions obtained by the linear stability analysis. In this case

$$\frac{\partial u'}{\partial x} + \frac{\partial w'}{\partial z} = 0 \quad (4)$$

therefore, by equation (3a)

$$A_x = A_z. \quad (5)$$

Also, the pressure term in equation (3b) may be shown to be identically zero.

3. EVALUATION OF THE AVERAGES IN THE POWER INTEGRAL EQUATIONS

Stuart's shape assumption [11] implies that u', w' and T' have the form

$$f' = (\mathrm{Re}[F] + \mathrm{Im}[F])(\cos\alpha x + \mathscr{s}\sin\alpha x) \quad (6)$$

where F denotes V, W and θ, functions of z only, and α is the x-spatial wavenumber. The real parts of the perturbation quantities have the form

$$\mathrm{Re}[f'] = \mathrm{Re}[F]\cos\alpha x - \mathrm{Im}[F]\sin\alpha x. \quad (7)$$

Interpreting the primed quantities in equations (3) as real parts, a general expression for all x averages is

$$\langle f'g'\rangle = \langle \mathrm{Re}[F]\,\mathrm{Re}[G]\cos^2\alpha x + \mathrm{Im}[F]\,\mathrm{Im}[G]\sin^2\alpha x - (\mathrm{Re}[F]\,\mathrm{Im}[G] + \mathrm{Re}[G]\,\mathrm{Im}[F])\cos\alpha x\sin\alpha x\rangle. \quad (8)$$

Performing the averages over any integral number of periods in x yields the expression

$$\langle f'g'\rangle = \tfrac{1}{2}\{\mathrm{Re}[F]\,\mathrm{Re}[G] + \mathrm{Im}[F]\,\mathrm{Im}[G]\}. \quad (9)$$

Defining the integrals in Table 1, where $D \equiv d/dz$, it follows that

$$A_z Gr\sin\phi\, c_1 + \frac{A_z^3}{2}c_2 - \frac{PrGr\sin\phi\, A_T A_z^2}{2} \times c_3 + A_z I_3 - GrA_T(\sin\phi I_1 + \cos\phi I_2) = 0 \quad (10a)$$

and

$$\frac{Pr^2 A_z^2 A_T}{2}c_4 - PrA_z I_2 + A_T I_9 = 0 \quad (10b)$$

where

$$c_1 = I_4 - I_5/24,$$
$$c_2 = I_8 - I_5^2,$$
$$c_3 = I_6 - I_5 I_7 - I_2 c_1$$

and

$$c_4 = I_{10} - I_2^2.$$

If the nonlinear terms are dropped from equations (10), the critical condition should be recovered. In this case

$$A_z Gr_c\sin\phi c_1 + A_z I_3 - Gr_c A_T \times \sin\phi\, I_1 - Gr_c A_T\cos\phi\, I_2 = 0 \quad (11)$$

and

$$A_T I_9 - Pr\,A_z I_2 = 0. \quad (12)$$

It follows that

$$Gr_c = I_3 I_9\{Pr(\sin\phi I_1 I_2 + \cos\phi I_2^2) - \sin\phi c_1 I_c\}. \quad (13)$$

Utilizing this expression, equations (10) may be solved for A_z and A_T with the results

$$S_1 A_z^4 + (S_2 + GrS_3)A_z^2 + \left(1 - \frac{Gr}{Gr_c}\right) = 0. \quad (14)$$

where

$$S_1 = \frac{Pr^2}{4}\frac{c_2 c_4}{I_3 I_9} \quad (15a)$$

$$S_2 = \frac{Pr^2}{2}\frac{c_4}{I_9} + \frac{c_2}{2I_3} \quad (15b)$$

and

$$S_3 = \frac{Pr^2}{2}\frac{\sin\phi(c_1 c_4 - I_2 c_3)}{I_3 I_9} \quad (15c)$$

and

$$A_T = \frac{PrA_z I_2}{I_9 + Pr^2 A_z^2 c_4/2}. \quad (16)$$

The preceeding analysis is similar to that of Gotoh and Ikeda [10]; however, the original form of the equations, and the details of the technique utilized in [10], ensure that the two analyses were performed independently. It is therefore of interest that, after considerable algebraic manipulation, it may be shown that equations (4.2) of [10] and the present equations (14) and (16) are equivalent.

4. SOLUTIONS

The solutions to equation (14) are

$$A_z = \pm\sqrt{\left[\left(-(S_2 + GrS_3) \pm \left\{(S_2 + GrS_3)^2 - 4S_1\left(1 - \frac{Gr}{Gr_c}\right)\right\}^{1/2}\right)\Big/ 2S_1\right]}. \quad (17)$$

Only the real values of A_z are of interest. Since $Gr > Gr_c$ in all cases where multi-cellular convection occurs.

and assuming $S_1 > 0$ (calculations for all ϕ and Pr support this assumption) then the argument of the inner root is always larger than 0. It follows that the inner root will always exceed in magnitude $(S_2 + GrS_3)$; therefore, in order that A_z be real, the positive sign of the inner root must be chosen. Taking the positive sign of the outer root as the preferred one (choosing the negative sign does not alter the analysis), it follows that the expression

$$A_z = \sqrt{\left[\left(-(S_2+GrS_3)+\left\{(S_2+GrS_3)^2 - 4S_1\left(1-\frac{Gr}{Gr_c}\right)\right\}^{1/2}\right)\Big/2S_1\right]} \quad (18)$$

gives the real values of A_z.

The heat transfer, in terms of the Nusselt number, Nu, is

$$Nu = \left.\frac{\mathrm{d}(T_b + T_a)}{\mathrm{d}z}\right|_{-1/2} \quad (19)$$

From equation (2a) and the boundary conditions, it follows that

$$Nu = 1 + \frac{PrA_TA_z}{2} I_2. \quad (20)$$

5. THE ENERGETICS

If equation (11) is considered in light of its derivation, the various terms may be identified with terms in the original equations. Hence, the first term arises from the base-flow term (convection), the second from the viscous term (dissipation), the third from the upslope buoyancy term (parallel buoyancy) and the last from the cross-stream buoyancy term (perpendicular buoyancy). These terms indicate the energy that each mechanism contributes to the instability. It is customary to scale these energies by assigning the dissipation term the value -1; this is achieved by dividing equation (11) by $-A_zI_3$. The result is

$$-Gr_c \sin\phi \frac{c_1}{I_3} - 1 + Gr_c \frac{A_T}{A_z} \sin\phi \frac{I_1}{I_3} + Gr_c \frac{A_T}{A_z} \cos\phi \frac{I_2}{I_3} = 0. \quad (21)$$

Using equation (12) to remove the A_T/A_z term, it follows that

$$-Gr_c \sin\phi \frac{c_1}{I_3} - 1 + Gr_cPr \sin\phi \frac{I_1I_2}{I_3I_9} + Gr_cPr \cos\phi \frac{I_2I_2}{I_3I_9} = 0. \quad (22)$$

Table 1. Integrals

Integral	Definition
I_1	$\int_{-1/2}^{1/2} \{\mathrm{Re}\,[U]\,\mathrm{Re}\,[\theta] + \mathrm{Im}\,[U]\,\mathrm{Im}\,[\theta]\}\,\mathrm{d}z$
I_2	$\int_{-1/2}^{1/2} \{\mathrm{Re}\,[W]\,\mathrm{Re}\,[\theta] + \mathrm{Im}\,[W]\,\mathrm{Im}\,[\theta]\}\,\mathrm{d}z$
I_3	$\int_{-1/2}^{1/2} \{\alpha^2 (\mathrm{Re}\,[U]^2 + \mathrm{Im}\,[U]^2 + \mathrm{Re}\,[W]^2 + \mathrm{Im}\,[W]^2) + (D\,\mathrm{Re}\,[U])^2 + (D\,\mathrm{Im}\,[U])^2 + (D\,\mathrm{Re}\,[W])^2 + (D\,\mathrm{Im}\,[W])^2\}\,\mathrm{d}z$
I_4	$\int_{-1/2}^{1/2} (r_3^2/2)\,\{\mathrm{Re}\,[W]\,\mathrm{Re}\,[U] + \mathrm{Im}\,[W]\,\mathrm{Im}\,[U]\}\,\mathrm{d}z$
I_5	$\int_{-1/2}^{1/2} \{\mathrm{Re}\,[W]\,\mathrm{Re}\,[U] + \mathrm{Im}\,[W]\,\mathrm{Im}\,[U]\}\,\mathrm{d}z$
I_6	$\int_{-1/2}^{1/2} \left\{\left(\mathrm{Re}\,[W]\,\mathrm{Re}\,[U] + \mathrm{Im}\,[W]\,\mathrm{Im}\,[U]\right) \int_0^\xi \int_0^\eta (\mathrm{Re}\,[\theta]\,\mathrm{Re}\,[W] + \mathrm{Im}\,[\theta]\,\mathrm{Im}\,[W])\,\mathrm{d}\eta\,\mathrm{d}\xi\right\}\mathrm{d}z$
I_7	$\int_{-1/2}^{1/2} \int_0^\xi \int_0^\eta \{\mathrm{Re}\,[\theta]\,\mathrm{Re}\,[W] + \mathrm{Im}\,[\theta]\,\mathrm{Im}\,[W]\}\,\mathrm{d}\eta\,\mathrm{d}\xi\,\mathrm{d}z$
I_8	$\int_{-1/2}^{1/2} \{\mathrm{Re}\,[W]\,\mathrm{Re}\,[U] + \mathrm{Im}\,[W]\,\mathrm{Im}\,[U]\}^2\,\mathrm{d}z$
I_9	$\int_{-1/2}^{1/2} \{\alpha^2[(\mathrm{Re}\,[\theta])^2 + \mathrm{Im}\,[\theta])^2] + (D\,\mathrm{Re}\,[\theta])^2 + (D\,\mathrm{Im}\,[\theta])^2\}\,\mathrm{d}z$
I_{10}	$\int_{-1/2}^{1/2} \{\mathrm{Re}\,[\theta]\,\mathrm{Re}\,[W] + \mathrm{Im}\,[\theta]\,\mathrm{Im}\,[W]\}^2\,\mathrm{d}z$

The terms of this equation are known as the energetics. Individually they are denoted by

$$E_D = -1$$

the energy dissipated by viscosity (23a)

$$E_C = -Gr_c \sin\phi\,(c_1/I_3)$$

the energy obtained from the mean velocity field (23b)

$$E_{\parallel} = Gr_c Pr \sin\phi\,(I_1 I_2/I_3 I_9)$$

the energy obtained from the parallel-buoyancy field (23c)

$$E_{\perp} = Gr_c Pr \cos\phi\,(I_2 I_2/I_3 I_9)$$

the energy obtained from the perpendicular-buoyancy field. (23d)

A physical interpretation of the energetics may be obtained by examining the definitions of I_i. Using Table 1, it may be seen that I_1 is the power extracted by u' from the T' field, I_2 is the power extracted by w' from the T' field, I_3 is the viscous power dissipation, and c_1 is the power extracted from the base flow. The E_C therefore indicates the fraction of the dissipation energy which is derived from the base flow. For all conditions studied, the factor PrI_2/I_7 was found to be identically 1.0; therefore, the $E_{\parallel}$ and $E_{\perp}$ indicate the fraction of the dissipation energy which is derived from the parallel buoyancy, due to the perturbation, and from the perpendicular buoyancy, due to the perturbation, respectively.

6. THE LIMITS

It is informative to study the limiting behaviour of dNu/dGr as $Gr \to Gr_c$ and Nu as $Gr \to \infty$. The first limit will indicate how rapidly convection grows, while the second limit will indicate how important the first mode of instability ultimately becomes. The two limits thereby provide an indication of the physical importance of the instability. By taking the limits, it may be shown that as $Gr \to Gr_c$

$$\frac{dNu}{dGr} \to \frac{Pr^2 I_2 I_2}{2Gr_c(S_2 + Gr_c S_3) I_9} \tag{24}$$

and as $Gr \to \infty$

$$Nu \to 1 + \frac{I_2 I_2}{c_4}. \tag{25}$$

7. RESULTS

7.1. *Introduction*

Solutions were obtained for the combinations of ϕ and Pr outlined in [1] and [2]. Some difficulty, however, arose for the higher values of ϕ and Pr. If the computer program used to solve for the desired parameters is functioning properly, equation (13) should yield values for Gr_c which are identical to those obtained by the linear stability analysis. In almost all cases agreement was obtained to at least eight figures. However, for $\phi > 30°$ and $Pr > 4$, the two sets of values began to diverge. Attempts to remedy this situation met with only limited success.

During preliminary program runs, it was found that, in order for the two values of Gr_c to agree, approximately twice the number of terms had to be used in the power series for the power integral technique as in the power series for the linear stability solution. This meant that for high ϕ and Pr, up to 400 terms were used in the case of the power integral technique. It was suspected that these long series, when used in multiplications and/or integrations, caused round-off errors, which lead to inexact results. In order to check this possibility, the parts of the program which utilized real arithmetic was converted to double precision (unfortunately a large part of the program required complex arithmetic which the CDC machine used did not support). The improvement in the results is illustrated in Table 2 for selected Prs and $\phi = 90$. Clearly the use of double precision gives significantly better results; however, the effects of these precision problems would be far more important in integrals which arise in the nonlinear terms, but are not present in the integrals used to determine Gr_c. Since there was no way to determine if round-off error was indeed affecting these higher order integrals, results which depended on them were generally not calculated for $Pr > 3.0$.

The precision problem discussed above does not seriously restrict the application of the power integral technique. As shown by Korpela, Gozum and Baxi [12], stationary transverse rolls are not the preferred mode of instability for $Pr > 12.7$; therefore, the region of interest which the present program cannot analyse is very limited. It is unfortunate, however, that water, one of the most important experimental fluids, happens to have Prs within this region.

Table 2. Effect of precision on the power integral analysis

Pr	Linear stability results	Power integral results (single precision)	Power integral results (double precision)
4.0	7859.3711	7836.0988	7859.3711
5.0	7863.9424	8312.2509	7863.9424
6.0	7866.6691	8880.0722	7866.6690

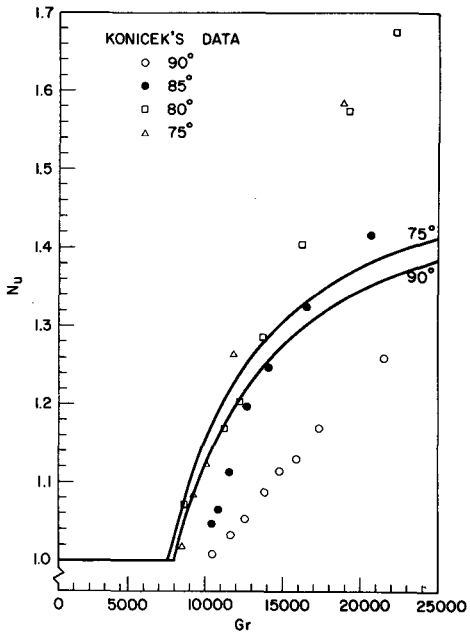

FIG. 1. Comparison with experiments (—— present theory; ○, ●, □, △ Konicek [9]).

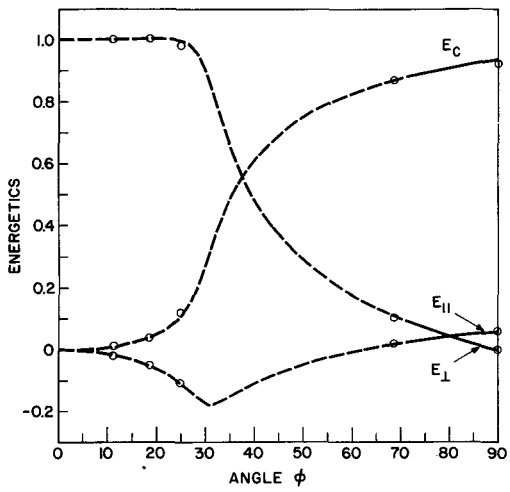

FIG. 2. Energetics for $Pr = 0.71$ (○ Hart [5]).

7.2. *Comparison of results with experiments*

Figure 1 shows a comparison between the predicted *Nu–Gr* behaviour, for the angles at which transverse rolls are expected in air, and the experimental results of [9]. The present predictions show little change over the range $75° \leq \phi \leq 90°$; the experimental results, however, show considerable variation. While the expermental results for $\phi = 75°$ and 80° agree quite well with the present predictions in the range $Gr_c \leq Gr \leq 12\,000$, the $\phi = 85°$ results show marked discrepancies near Gr_c but good agreement (possibly fortuitous) for $12\,000 \leq Gr \leq 16\,000$. The $\phi = 90°$ results seem to imply that an entirely different mode of behaviour exists at that angle. These results may imply that the vertical temperature gradient is very important at $\phi = 90°$ but rapidly loses its importance as the angle decreases. Obviously, more experimental work is needed before anything conclusive can be said about this problem. The rise of the data above the predictions is similar to that which ocurs in the case of longitudinal rolls at low angles (see [13]). In the region immediately after the onset of multi-cellular convection, the behaviour of the experimental data and the present predictions are clearly similar, at least for the two lower angles considered. This agreement was interpreted as a tentative confirmation of the applicability of the power integral technique.

7.3. *The energetics for* Pr = 0.71

Figure 2 shows the presently calculated energetics for $Pr = 0.71$. As in [2], predictions for which transverse rolls will not physically obtain, since longitudinal rolls have a lower Gr_c, are plotted as dashed curves; transverse rolls physically occur only for predictions plotted as solid curves. Hart's results [5], obtained by the Galerkin method, are plotted for comparison. Agreement between the two sets of results is excellent; this provides a further validation of the present technique. The trends of the curves may be understood by considering the arguments given in the next section, where the behaviour of the energetics for $0 \leq Pr \leq 10$ is discussed.

7.4. *The energetics as functions of the* Pr

The energetics are presented as functions of *Pr* in Fig. 3. The most striking feature is the *Pr* effect at low ϕ. For $Pr < 1$, the energetics of the instability quickly approach those for $Pr = 0$, even at angles as low as 10°. This indicates that, at low *Pr* and $\phi \neq 0$, the instability always gains all of its energy from the base flow (a shear instability).

The behaviour of the energetics may be explained by means of arguments based on a physical interpretation of the energetics and on *Pr* effects. The energetics imply three sources of energy for the instability: the perpendicular buoyancy due to the temperature perturbation, the parallel buoyancy due to the temperature perturbation and the mean thermal field which supplied energy to the instability via the mean velocity field; the *Pr* gives an indication of the relative importance of viscous dissipation as compared to thermal dissipation.

At very low *Pr*, the thermal dissipation greatly exceeds the viscous dissipation. This means that any purely thermal perturbations will be quickly dissipated. However, since viscosity is low, velocity disturbances may grow. Hence, at low *Pr*, the source of instability energy must be the base flow, as indicated by the energetics. At low *Pr*, the thermal diffusivity is so great that this energy may be supplied by allowing a

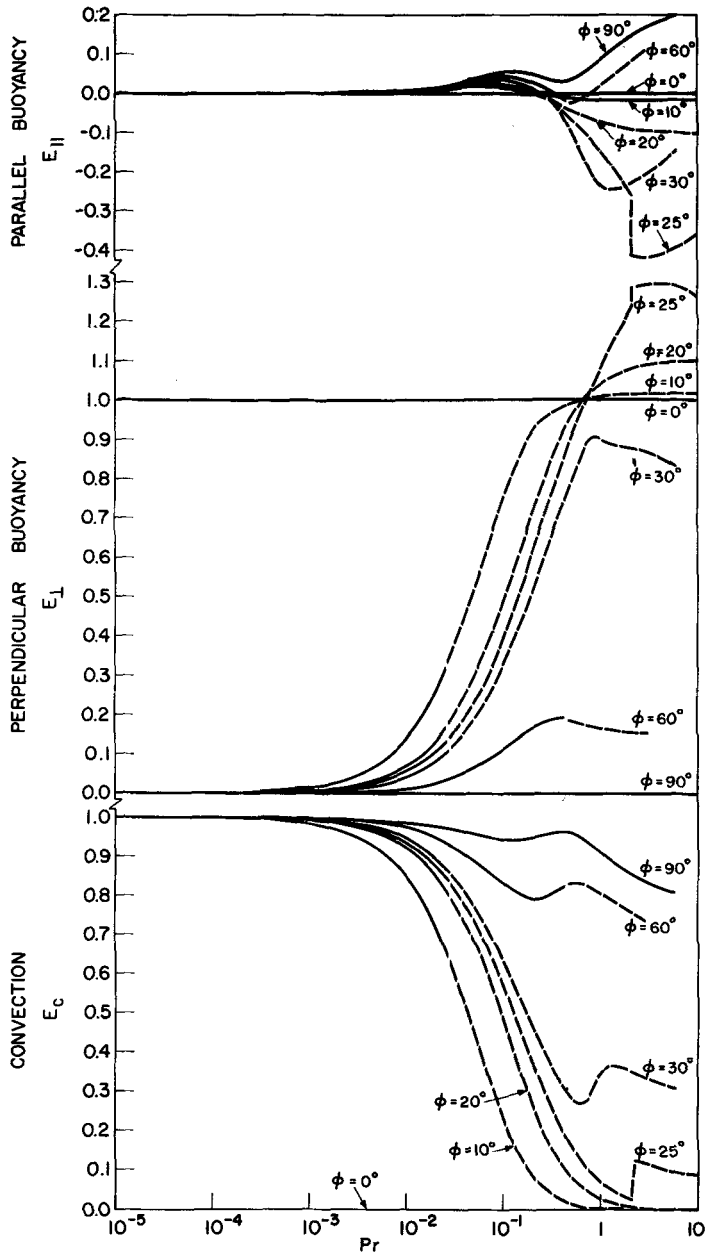

FIG. 3. Energetics at instability.

very small (even infinitesimal) change in the mean temperature field. It may be seen therefore, that, although the instability is classified as a shear instability, the energy source is still ultimately thermal; the energy which is taken from the mean flow must ultimately be provided by a slightly altered mean thermal field. However, no energy is gained directly from the thermal perturbations. Of course when $\phi = 0°$, no base flow exists, and the instability does not occur until conditions are such that the perpendicular buoyancy can supply sufficient energy to maintain the instability. This explains why the $\phi = 0°$ results are anomalous at low Pr; for even a very small angle and Pr small but not 0, base flow exists and may therefore be an energy source for the instability.

As the Pr increases, thermal dissipation becomes less dominant and thermal perturbations are allowed to grow. The energy for the instability may then be supplied directly from the perturbations rather than by the mean temperature field. There is, however, an essential difference between a thermal disturbance occurring at low angles and one occurring at high angles. Assume that a positive temperature perturbation occurs at a point in the fluid layer. The perturbed particle will rise in the direction opposite to gravity. At low angles, this will quickly bring it into a

region of lower average temperature (recall the negative gradient base temperature in the fluid layer) which will increase its buoyant effect. At high angles, however, the particle will require a considerably longer travel before it reached areas of similar lower temperature, simply because at higher angles the gravity vector is more parallel to x along which there is no average thermal gradient. A perpendicular buoyancy perturbation is therefore inherently able to supply more energy to the instability than a parallel buoyancy perturbation.

As well as a decrease in thermal dissipation, an increase in Pr implies an increase in viscous dissipation and a shear instability is therefore more difficult to maintain. For low angles ($\phi < 25°$), Fig. 3 shows that the shear instability present at $Pr = 0$ loses all importance as $Pr \to \infty$. It would appear that the increase in viscous dissipation nullifies the shear type instability but is insufficient to suppress the instability driven by the strong perpendicular buoyancy.

For $\phi < 25°$, the behaviour of $E_{\|}$ is very interesting. As the Pr increases from zero, the parallel buoyancy becomes first an energy source, of quite low strength, then, at $Pr \simeq 0.25$, it becomes an energy sink. An inspection of the detailed results for the values of the integrals showed that, at the point where $E_{\|}$ becomes negative, the value of I_1 also becomes negative. By inspecting Table 1, it may be seen that this negative sign implies that u' and T' are out of phase. Provided u' and T' are in phase, the temperature perturbation will yield a buoyancy which will assist in maintaining the instability; the parallel buoyancy would then act as an energy source. However, when u' and T' are out of phase, the parallel buoyancy provides a force which opposes the motion; the parallel buoyancy then acts as an energy sink. For $\phi = 10°$ and $20°$, $E_{\|}$ continues to become more negative as Pr increases. The explanation for the behaviour of $E_{\|}$ at these low angles is probably that here the parallel buoyancy is too weak (recall the earlier arguments) to seriously affect the solution. The initial rise of $E_{\|}$ may simply occur because of the combined effects of the shear instability and the perpendicular buoyancy; when the perpendicular buoyancy dominates the behaviour of the instability, it would appear that it gives rise to the parallel buoyancy becoming an energy sink.

The discontinuous behaviour of the energetics at $\phi = 25°$ indicates the transition to a new type of energy balance. Figure 4 contains some new results for Gr_c at $\phi \simeq 25°$. These results show that the transition at $\phi = 25°$ occurs abruptly, that is, two modes of instability co-exist over a range of Pr and the transition from one mode to the other comes about because the solution for the mode with the lower Gr_c ceases to exist past a certain Pr. (These results were obtained by the technique of [1] and [2]. The method was to search for Gr_c by taking small steps in Pr and using the previous value of Gr_c as the initial guess. Searches were done for both increasing Pr and decreasing Pr as indicated in the figure by the arrows.) The reason for this transition is as follows. As the angle increases, the perpendicular buoyancy, which depends on the $\cos\phi$, decreases; at the same time the parallel buoyancy becomes an increasingly strong energy sink. In addition, as Pr increases, viscous dissipation increases; therefore, more energy is needed to maintain the instability. An untenable situation now arises; the instability derives almost all its energy from the perpendicular buoyancy (which is decreasing with increasing angle), while it is being increasingly resisted by the parallel buoyancy (which is increasing with increasing angle); meanwhile, the viscous dissipation is increasing with Pr. A

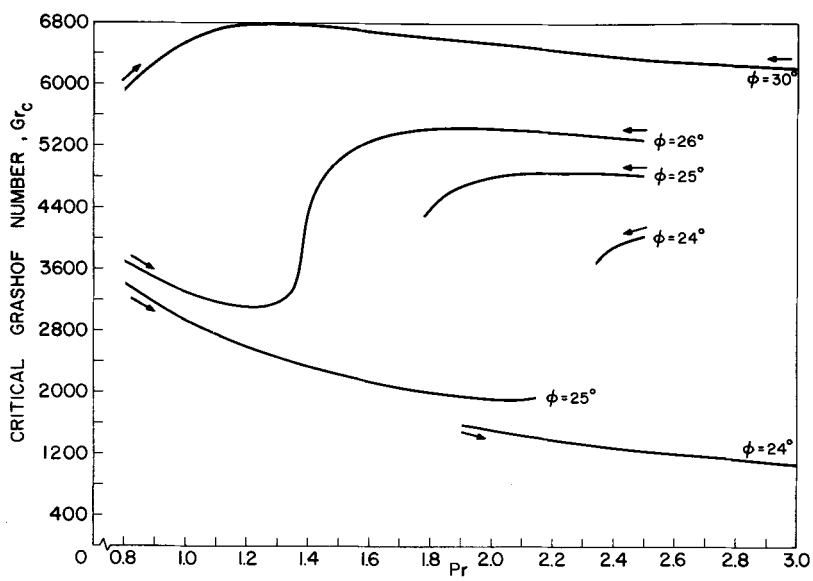

FIG. 4. Behaviour of Gr_c with Pr around $\phi = 25°$.

Pr–ϕ point is reached where the perpendicular buoyancy simply cannot maintain motion and the low angle type solution ceases to exist; the remaining higher Gr_c instability, which admits both a larger energy contribution from the base flow and an entirely new energy balance, is then the only remaining mode of instability.

The results in Fig. 4 indicate that the discontinuous change in the mode of instability occurs only for $\phi = 25°$. For $\phi = 24°$, at least in the Pr range considered, the change of mode does not occur, while for $\phi \simeq 26°$ the change is continuous, albeit rapid. The reason for continuous change at angles higher than $\phi = 25°$ may be that at the higher angles the perpendicular buoyancy is reduced sufficiently that the viscous dissipation can effect a gradual transition at a Pr low enough that the thermal dissipation is still sufficiently strong to help control the thermal disturbance.

As the angle increases, the $Pr = 0$ type shear instability is manifest at increasing values of Pr. The reason for this is that, as the angle increases, the perpendicular buoyancy diminishes while the parallel buoyancy increases; but, as described above, the parallel buoyancy is inherently a weaker source of energy for the instability. Therefore, the instability must depend more on the energy from the mean field to support it. This reasoning also explains why the minimum which occurs in E_C near $Pr = 1$ shifts to the left with ϕ; since the parallel buoyancy is weaker than the perpendicular buoyancy, viscous dissipation, which increases with increased Pr, is more effective in suppressing an instability driven by parallel buoyancy.

The only trend in the energetics not yet explained is the decrease in E_c, for $\phi \geq 25°$, as $Pr \to 10$. The explanation for this is simply that, as $Pr \to \infty$, the problem approaches an adiabatic limit. At this limit, a temperature disturbance would act as an adiabatic buoyant particle; since the thermal disturbance would not propagate, it would not cause a cellular structure to form. The result would be a thermal disturbance which would cause a motion which in turn would be quickly damped out by viscosity. Also, at an adiabatic limit, the mean thermal field could not supply energy to maintain a shear type instability. Therefore, at high angles and high Pr, a perturbation will have difficulty maintaining itself (this argument would suggest that at high angles and Pr, the ultimate effect of the instability on Nu should be greatly reduced). The reason that the point where the near adiabatic behaviour becomes manifest (the high Pr maximum of the $\phi \geq 25°$ curves) shifts to lower Pr as ϕ increases is that the parallel buoyancy becomes stronger as ϕ increases. (It should be kept in mind that at the Prs considered no truly adiabatic behaviour is exhibited; however, the concept of an adiabatic limit is still valid.)

In summary, the following regimes of behaviour may be identified:

(a) For small Pr and $\phi \neq 0$, E_C is 1.0. This is due to the large thermal dissipation and the virtual absence of viscous dissipation. This regime will be termed the shear regime.

(b) For $\phi < 25°$ and Pr large, $E_C \to 0$. This is due to the fact that the perpendicular buoyancy is so strong that it dominates over all other forces. This regime will be termed the thermally buoyant regime.

(c) For all angles, as Pr is increased from 0, E_C gradually decreases, while $E_\perp$ and/or $E_\parallel$ gradually increase. This is due to the decreased thermal dissipation at moderate Pr which in turn allowed thermal perturbations to be maintained. This regime is part of the thermally buoyant regime.

(d) For $\phi \geq 25°$, as Pr is increased further, E_C increases. This is due to the increased viscous effects, and consequently, the necessary increase in importance of the mean thermal field. This regime will be termed the viscosity controlled regime.

(e) For $\phi \geq 25°$, as Pr is increased still further, E_C decreases and $E_\parallel$ increased. This is due to the approach to a near adiabatic, parallel buoyant instability. This regime will be termed the adiabatically buoyant regime.

It is of considerable interest that the extrema of the E_C curves correspond exactly with the respective extrema of the Gr_c curves presented in [2]. The above arguments therefore explain the variations of Gr_c with Pr presented there. In the shear regime, thermal perturbations are damped, and the instability does not set in until the magnitude of the base flow is sufficiently large to overcome the viscous damping; velocity perturbations may then grow. In the thermally buoyant regime, the thermal dissipation becomes decreasingly less efficient as a damper of thermal disturbances; hence, thermal perturbations grow more easily and Gr_c decreases. At $Pr \simeq 1$, viscous dissipation becomes more dominant; hence, the thermal disturbances must be stronger to cause instability. But, as ϕ increases the buoyancy strength decreases; therefore, at higher angles the instability will be delayed until Gr_c increases sufficiently to overcome the increased viscous forces. This gives rise to the viscosity controlled regime. Finally, at high Pr and ϕ, the adiabatically buoyant regime exists. In this regime, the thermal perturbation cannot be effectively damped by thermal dissipation; therefore, it becomes an 'irresistible' force. This leads to a decrease in Gr_c. The fact that solutions for the critical conditions are hard to find at high ϕ and for $Pr > 10$ is probably explained by the fact that at high Pr and ϕ the parallel buoyancy acts as an 'irresistible' force, while due to viscosity, the buoyant particle acts as an 'immovable' object. The result is that any possible disturbance is of small magnitude; hence it is hard to predict accurately.

7.5. *The limiting results*

The results for the two limits discussed in Section 6 are presented in Figs. 5 and 6. The single result of [10] is plotted in Fig. 5 for comparison. Unfortunately, there are not present predictions for the Pr and ϕ considered by those workers; however, their datum is consistent with the curves here presented. (It is noted in passing that the stability criterion given by [10] was

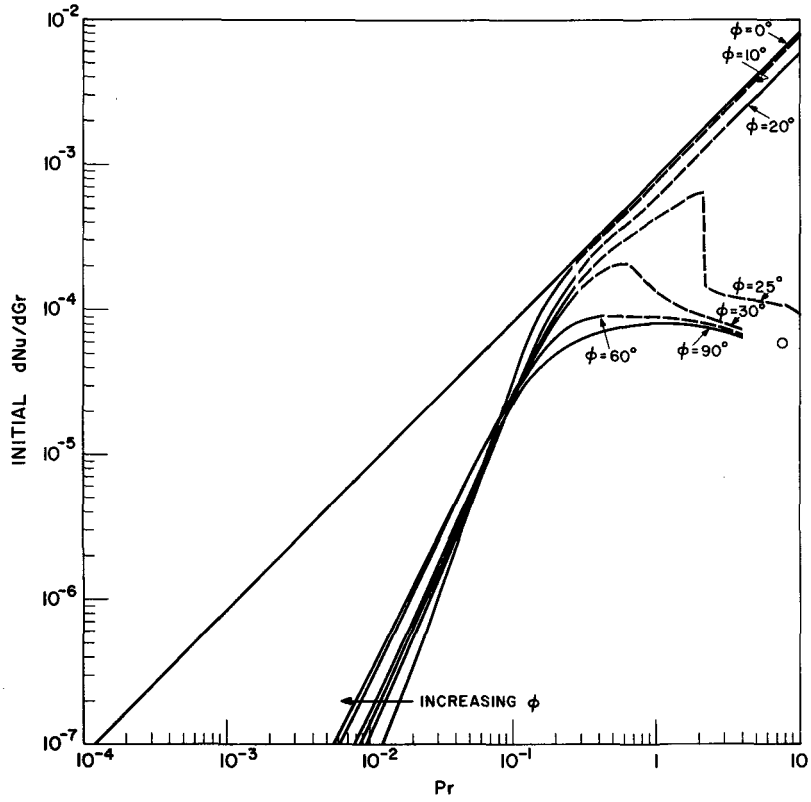

FIG. 5. Behaviour of dNu/dGr as $Gr \to Gr_c$ (○ Gotoh and Ikeda [10], $\phi = 90°$).

independently checked by the method of [1]. The previous and the present values are 7876.9557 and 7876.9584 respectively, agreement to 6 places.)

The limit results give an indication of the effect of ϕ and Pr on the relative importance of the instability to the heat transfer. For low Pr, Fig. 5 shows that the rate of increase of heat transfer with Gr is very small; hence, the heat transfer is little affected by the instability. For $\phi > 0$, Fig. 5 further indicates that the growth rate decreases with increasing angle for $Pr > 0.09$ and increases with increasing angle for $Pr < 0.09$. The behaviour of the $\phi = 0°$ data is clearly anomalous; for $Pr < 0.1$, the $\phi = 0°$ trend is not duplicated by any other angle. The ultimate influence of the instability is best measured as its maximum possible effect, that is, its effect as $Gr \to \infty$. Figure 6 indicates that, as Pr increases, the ultimate effect of the instability decreases. (This is consistent with arguments presented

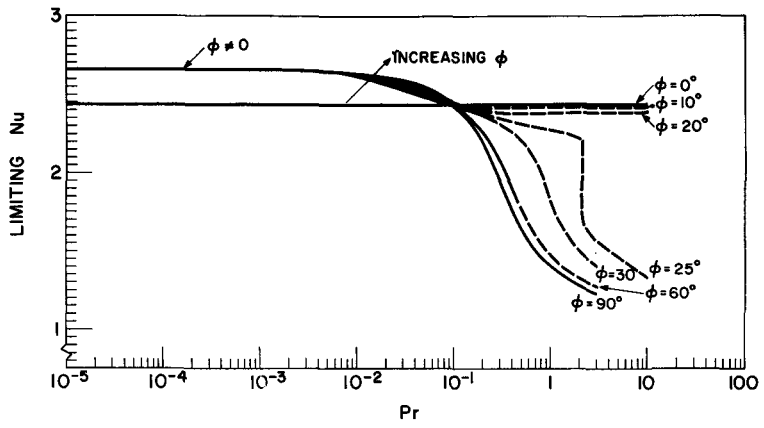

FIG. 6. Behaviour of the Nu as $Gr \to \infty$.

in the previous section.) As in the previous figure, as $Pr \to 0$, no angle gives results similar to those of $\phi = 0$. Furthermore, as the angle increases, the limiting value initially increases for $10^{-2} \leq Pr \leq 10^{-1}$ and significantly decreases at higher Prs. In fact, for $Pr = 3$ and $\phi = 90°$, the instability ultimately gives rise to a Nu increase on the order of 0.25, which is almost six-fold less than the ultimate effect of the instability in a horizontal layer. It is clear, therefore, that aside from the fact that the stationary transverse instability is not the preferred mode at higher Pr and ϕ, it would not be physically important even if it were the preferred mode.

8. CONCLUSIONS

The preceding work supports the following conclusions:

(1) The power integral technique, when coupled with power series stability solutions, provides a simple, efficient method of ascertaining the importance of hydrodynamic instabilities.

(2) A comparison of the present results with previous experimental data suggests that the 'vertical' temperature gradient, present in the core of inclined layers, is of importance only near $\phi = 90°$, at least for air.

(3) By means of Pr arguments, the energy balance of the instabilities has been explained for $0° \leq \phi \leq 90°$ and $0 \leq Pr \leq 10$. Four regimes of influence have been identified.

(4) The arguments presented to accomplish conclusion 3 also explains the behaviour of Gr_c within the same ϕ and Pr ranges.

(5) As $\phi \to 90°$ and $Pr \to 10$, the effect of the instability on the heat transfer diminishes.

Acknowledgements—This work was supported by an operating grant from the Natural Science and Engineering Research Council of Canada. The author would like to thank Dr T. E. Unny of the University of Waterloo for originally bringing this problem to his attention and for providing an unpublished manuscript on the subject. The author would also like to thank Dr K. G. T. Hollands and Dr G. D. Raithby of the Univerxity of Waterloo and Dr A. Pollard of the University of Calgary for discussions during the course of this work.

REFERENCES

1. D. W. Ruth, On the transition to transverse rolls in an infinite vertical fluid layer – a power series solution, *Int. J. Heat Mass Transfer* **22,** 1199–1208 (1979).
2. D. W. Ruth, On the transition to transverse rolls in inclined infinite fluid layers – steady solutions, *Int. J. Heat Mass Transfer* **23,** 733–737 (1980).
3. E. R. G. Eckert and W. O. Carlson, Natural convection in an air layer enclosed between two vertical plates with different temperatures *Int. J. Heat Mass Transfer* **2,** 106–120 (1961).
4. J. W. Elder, Laminar free convection in a vertical slot, *J. Fluid Mech.* **23,** 77–98 (1965).
5. J. E. Hart, Stability of the flow in a differentially heated inclined box, *J. Fluid Mech.* **47,** 547–576 (1971).
6. A. E. Gill, The boundary layer regime for convection in a rectangular cavity, *J. Fluid Mech.* **26,** 515–536 (1966).
7. G. D. Raithby, K. G. T. Hollands and T. E. Unny, Free convection heat transfer across fluid layers of large aspect ratios, ASME publication 76-HT-37 (1976).
8. R. F. Bergholz, Instability of steady natural convection in a vertical fluid layer, *J. Fluid Mech.* **84,** 743–768 (1978).
9. L. Konicek, Experimental determination of critical Rayleigh numbers and heat transfer through horizontal and inclined air layers, M.A.Sc. thesis, University of Waterloo (1971).
10. K. Gotoh and N. Ikeda, Secondary convection in a fluid between parallel vertical plates of different temperatures, *J. Phys. Soc. Japan* **33,** 1697–1705 (1972).
11. J. T. Stuart, On the non-linear mechanics of hydrodynamic stability, *J. Fluid Mech.* **4,** 1–21 (1958).
12. S. A. Korpela, D. Gozum and C. B. Baxi, On the stability of the conduction regime of natural convection in a vertical slot, *Int. J. Heat Mass Transfer* **16,** 1683–1690 (1973).
13. D. W. Ruth, K. G. T. Hollands and L. D. Raithby, On free convection experiments in inclined air layers heated from below, *J. Fluid Mech.* **96,** 461–479 (1980).

CONVECTION D'AMPLITUDE FINIE DANS DES FENTES INCLINEES OU VERTICALES: UNE ANALYSE INTEGRALE

Résumé — Une analyse intégrale est conduite pour l'étude de l'effet de l'angle et du nombre de Peclet sur le transfert thermique juste après l'instabilité convective dans des couches fluides inclinées ou verticales. La configuration admise est celle de rouleaux transversaux. L'énergétique de l'instabilité est en bon accord avec les résultats de Hart. La variation avec le nombre de Prandtl est utilisée pour expliquer la variation du nombre critique de Grashof avec le nombre de Prandtl. Le transfert thermique est en bon accord avec les données de Konicek et avec les travaux théoriques de Gotoh et Ikeda. Ces résultats suggèrent que le gradient vertical de température observé dans les couches verticales peut ne pas être aussi important dans les couches inclinées à $\phi \leqslant 80°$. L'effet de l'instabilité sur le transfert thermique diminue lorsque $\phi \to 90°$ et $Pr \to 10$.

KONVEKTION MIT ENDLICHER AMPLITUDE IN GENEIGTEN UND SENKRECHTEN SPALTEN

Zusammenfassung — Der Einfluß von Winkel und Prandtl-Zahl auf den Wärmeübergang knapp jenseits der Grenze der konvektiven Stabilität in geneigten und senkrechten Schichten wird untersucht. Die Konvektionsbewegung wird als querliegende Walze angenommen. Die energetischen Verhältnisse der Instabilität zeigen gute Übereinstimmung mit den von Hart veröffentlichten. Die Veränderung dieser Verhältnisse mit der Prandtl-Zahl wird dazu benutzt, die Änderung der kritischen Grashof-Zahl mit der Prandtl-Zahl zu erklären. Die Wärmeübergangsergebnisse zeigen gute Übereinstimmung mit einigen der Daten von Konicek und mit der theoretischen Arbeit von Gotoh und Ikeda. Diese Ergebnisse lassen vermuten, daß der senkrechte Temperaturgradient, der in senkrechten Fluidschichten beobachtet wird, in Schichten die um $\phi = 80°$ geneigt sind, von geringerer Bedeutung ist. Es zeigt sich, daß der Einfluß der Instabilität auf den Wärmeübergang geringer wird, wenn ϕ gegen 90° und Pr gegen 10 geht.

КОНВЕКЦИЯ КОНЕЧНОЙ АМПЛИТУДЫ В НАКЛОННЫХ И ВЕРТИКАЛЬНЫХ ЩЕЛЯХ. ИНТЕГРАЛЬНЫЙ МЕТОД

Аннотация — Интегральным методом изучено влияние угла наклона и числа Прандтля на теплоперенос после возникновения конвективной неустойчивости в наклонных и вертикальных слоях жидкости. Предполагается, что конвекция имеет форму поперечных валов. Показано, что пороги неустойчивости хорошо согласуются с опубликованными данными Харта. Изменения порогов неустойчивости в зависимости от числа Прандтля используются для объяснения изменения критического числа Грасгофа в зависимости от числа Прандтля. Результаты по теплообмену хорошо согласуются с экспериментальными данными Коничека и теоретическими работами Гото и Икеды. Данные результаты указывают на то, что вертикальный градиент температуры, наблюдаемый в вертикальных слоях жидкости, несущественен в слоях с углм наклона $\phi \leq 80°$. Показано, что влияние неустойчивости на теплообмен ослабевает по мере того, как $\phi \to 90$ и $Pr \to 10$.